BRIEF COMMENTS ON ELASTIC FLEXIBILITY OF REINFORCED CONCRETE FRAMES AND SIGNIFICANCE TO SEISMIC DESIGN

M.J.N. Priestley[1]

ABSTRACT

It is shown, from analysis of typical reinforced concrete beam sections, that current design practice, which assumes beam stiffness is independent of reinforcement ratio but equal to a constant fraction of gross section stiffness is inappropriate. The analyses indicate that effective beam yield curvature can be considered constant, when non-dimensionalized by beam depth and yield strain, indicating that beam stiffness is proportional to strength. Based on this observation, a simple expression for yield drift of frames is proposed and is calibrated by comparing with results of a large number of beam/column subassemblage experiments. Good agreement is obtained. It is pointed out that current estimates of frame stiffness are generally too high. A consequence is that simple calculations show that the vast majority of frame buildings will be unable to achieve code design ductility levels before exceeding code drift limitations.

INTRODUCTION

Recent extensive parameter studies of moment-curvature response of bridge columns [1] and structural walls [2] have shown that it is inappropriate to assume that the effective stiffness, I_e, including effects of cracking, is a constant proportion of gross section stiffness, I_g, regardless of reinforcement content and axial load level. The analyses indicated that yield curvature, defined as the curvature at first yield of tension reinforcement, or at an extreme fibre compression strain of 0.002, extrapolated to the nominal flexural strength M_n (see Fig. 1), is essentially independent of both longitudinal reinforcement ratio and axial load ratio over the practical design range of these parameters and can be expressed by the following dimensionless equations:

Circular columns	$\phi_y D = 2.35\,\varepsilon_y \pm 15\%$	(1a)
Rectangular columns	$\phi_y h_c = 2.12\,\varepsilon_y \pm 10\%$	(1b)
Structural walls	$\phi_y \ell_w = 2.0\,\varepsilon_y \pm 10\%$	(1c)

where D, h_c, and ℓ_w are the diameter, section depth, and wall length, respectively, and ε_y is the yield strain of the longitudinal reinforcement.

A consequence of this invariance of yield curvature is that the common design practice of allocating lateral forces between different seismic resisting elements in proportion to their stiffness is invalid, since strength and stiffness must be proportional, if the concept of constant yield curvature is accepted. This paradox is discussed in detail in reference [2].

YIELD CURVATURE FOR BEAM SECTIONS

The results for walls and columns would indicate that current practice for frames might also lead to significant errors. The New Zealand concrete code [3] recommends a value for beam stiffness of $I_e = 0.4\ I_g$ for rectangular sections, and $I_e = 0.35 I_g$ for T-beam sections. If, following trends for walls and columns, it were found that beam stiffness depended strongly on reinforcement content, and hence on strength, it might be expected that current calculations for building period, and for expected drift might be significantly in error.

In order to investigate the influence of reinforcement content on beam stiffness, the typical beam section of Fig. 2 was considered. Top and bottom reinforcement was placed in either one or two layers. Cover to main reinforcement was 40 mm, a bar size of D24 was assumed with 24 mm between layers. Tension reinforcement ratios, based on an effective depth of 548 mm were 0.82%, 1.54% or 2.2%. For top steel, these ratios were taken to include the effective slab contribution. Most analyses were for equal top and bottom reinforcement, though one case with 2.2% top reinforcement and 1.1% bottom reinforcement was considered. Reinforcement yield strength was either 300 MPa or 400 MPa, and a concrete compression strength of 30 MPa was assumed. Analyses were carried out for both negative (-ve, top steel in tension) bending, and positive (+ve, bottom steel in tension) bending.

Analyses were carried out using a specialized moment-curvature program that considers strain hardening effects, and confinement of concrete, where appropriate. The nominal flexural strength is determined at a curvature equal to 5 times

[1] *University of California, San Diego, California (Fellow and ex-President)*

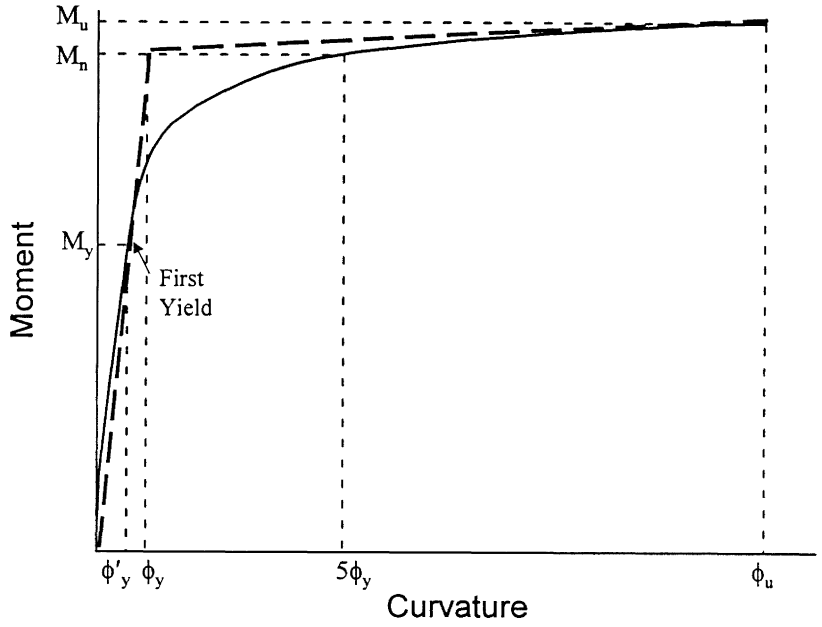

Figure 1: Effective bi-linear yield curvature

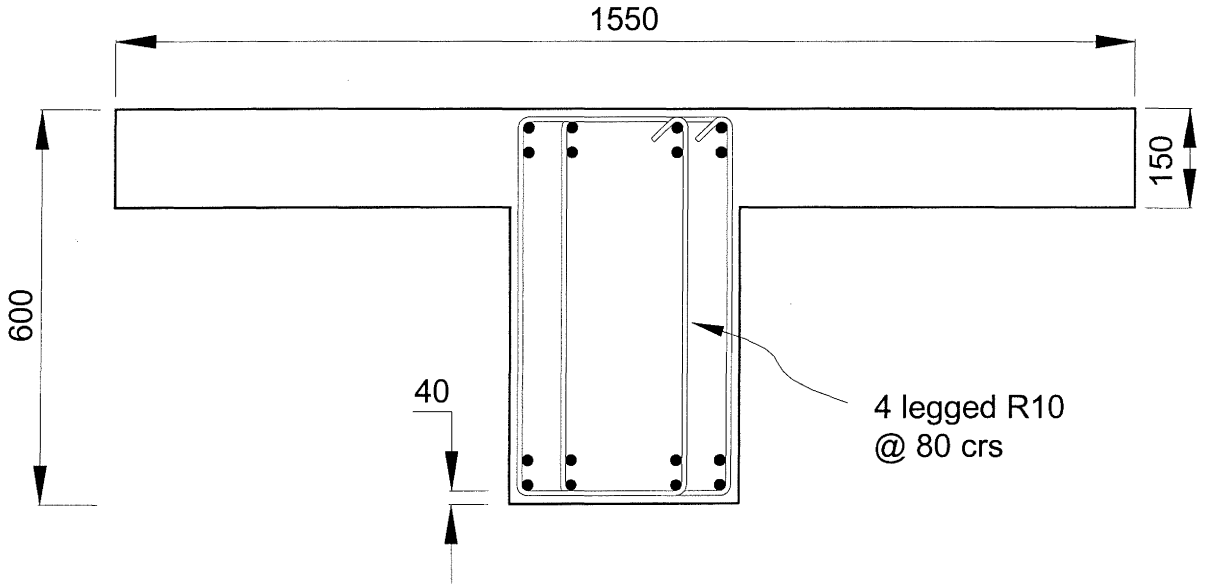

Note: All dimensions in mm

Figure 2: Section considered for moment-curvature analysis

the nominal biaxial yield curvature (see Fig. 1) which involves an iterative solution. Choosing this definition of nominal flexural strength rather than the more usual value corresponding to an extreme fibre compression strain of 0.003 or 0.004 avoids excessively high estimates of flexural strength of doubly reinforced sections when strain hardening is included in the analysis.

Results of the analyses are included in Tables 1 and 2. Table 1 lists the yield curvatures for both 300 and 400 MPa reinforcement, under the usual design assumption that strain hardening is ignored in the analysis for flexural strength. Also listed in Table 1 is the yield curvature for f_y = 400 MPa reinforcement where the nominal flexural strength includes the influence of strain hardening. Although not considered appropriate for force-based design, this assumption is relevant for frames designed to displacement-based principles [4]. For grade 400 reinforcement, strain hardening increases the nominal strength, as defined above, by up to 15%. For grade 300 reinforcement, with its longer yield plateau, the influence is negligible, and is hence not included in Table 1.

If an equation of the form of Eqn. (1) were appropriate for beams, we could write it as

$$\phi_y h_b = k\, \varepsilon_y \qquad (2)$$

where h_b = total beam depth [600 mm for Fig.1]. Table 1 thus includes the value

$$k = \phi_y h_b / \varepsilon_y \qquad (3)$$

where the yield strain is taken as 0.0015 and 0.0020 for f_y = 300 MPa and 400 MPa, respectively. For beam stiffness calculations, the average for negative and positive bending is appropriate as a consequence of moment reversal along the beam length under seismic loading conditions. Consequently, the averaged curvature and average value of k given by Eqn. (3) are also included for the five cases considered in Table 1.

Examination of Table 1 indicates that, for a given reinforcement strength, yield curvatures show comparatively minor variation, despite a moment range exceeding 250%, related to the lowest flexural strength (see Table 2). Also, when non-dimensionalized in accordance with Eqn. (3), the value of k for both 300 MPa and 400 MPa reinforcement varies within a narrow range, when strain hardening is ignored. Based on the average of positive and negative bending for each case, Eqn. (2) can be written as

$$\phi_y h_b = 1.7\, \varepsilon_y \qquad \pm 10\% \qquad (4a)$$

for the full range of cases considered. Including the effects of strain hardening would result in

$$\phi_y h_b = 1.9\, \varepsilon_y \qquad \pm 10\% \qquad (4b)$$

For rectangular-section beams rather than flanged beams, the negative bending results would be applicable for both negative and positive bending, resulting in average values of k about 10% higher, and with slightly increased scatter. It would thus appear that the concept of a constant dimensionless yield curvature for beam sections is an adequate approximation.

Table 2 lists nominal flexural strengths M_n for the different cases analyzed. The effective stiffness can be calculated from the so-called "beam equation" as

$$E_c I_e = \frac{M_n}{\phi_y} = \frac{M_y}{\phi_y'} \qquad (5)$$

Hence,

$$I_e = \left[\frac{M_n}{\phi_y E_c I_g}\right] I_g \qquad (6)$$

where I_g is the gross moment of inertia (0.01155 m^4 for the section of Fig.1). Table 2 also lists the factor in parentheses in Eqn. (6) based on E_c = 30 GPa. It will be observed that the average I_e for the five cases considered varies between 16% and 44% of I_g, with a wider range applicable if negative and positive bending are connected separately. It is thus clear that even if an average value of 30% I_g is adopted, errors in stiffness up to 50% can be expected for the range of cases considered. With higher or lower reinforcement ratios, which are possible, the errors would be even greater. Using typical design values of 35% to 40% I_g, as proposed in [3], errors are likely to be larger, with most designs being significantly more flexible than assumed.

YIELD DRIFTS FOR FRAMES

The comparitive invariance of nondimensional yield curvature developed above indicates that yield drift of frames might similarly be essentially independent of reinforcement ratio and strength. Fig. 3(a) shows a typical beam/column subassemblage extending half a bay width either side of the joint and half a storey height above and below the joint. Since bay width will normally exceed storey height, and column curvatures will typically be less than beam curvatures as a consequence of capacity design procedures, beam flexibility is likely to dominate the deformation.

The deflected shape is shown in Fig. 3(b). The yield drift θ_y can be expressed as

$$\theta_y = \theta_{by} + \theta_{jy} + 2\Delta_c / \ell_c + 2\Delta_s / \ell_c \qquad (7)$$

where θ_{by} = rotation of the joint center due to beam flexure,

θ_{jy} = joint shear rotation,

Δ_c = deflection of column top relative to tangent rotation at joint centre,

TABLE 1: YIELD CURVATURES FOR DIFFERENT BEAM REINFORCEMENT DETAILS

REIN-FORCEMENT	BENDING CASE	f_y=300 MPa		f_y =400 MPa		f_y =400 MPa, STRAIN HARDENING	
		ϕ_Y X 1000m^{-1}	$h_B\phi_Y/\varepsilon_Y$	ϕ_Y X 1000m^{-1}	$h_B\phi_Y/\varepsilon_Y$	ϕ_Y X 1000m^{-1}	$h_B\phi_Y/\varepsilon_Y$
0.82% top & bottom single layer	-ve	4.14	1.66	5.24	1.57	6.21	1.86
	+ve	3.88	1.55	4.95	1.49	5.68	1.70
	Average	4.01	1.61	5.10	1.53	5.95	1.78
1.54% top & bottom single layer	-ve	4.44	1.78	5.71	1.71	6.74	2.02
	+ve	3.90	1.56	4.98	1.49	5.68	1.70
	Average	4.17	1.67	5.35	1.60	6.21	1.86
2.2% top & bottom single layer	-ve	4.65	1.86	6.08	1.83	7.16	2.15
	+ve	3.88	1.55	5.13	1.54	5.87	1.76
	Average	4.27	1.77	5.61	1.69	6.52	1.95
2.2% top & bottom two layers	-ve	4.95	1.98	6.54	1.96	7.65	2.30
	+ve	4.31	1.72	5.36	1.61	6.10	1.83
	Average	4.63	1.85	5.95	1.78	6.88	2.07
2.2% top 2 layers 1.1% bottom (1 layer)	-ve	5.25	2.10	7.03	2.11	8.01	2.40
	+ve	3.66	1.46	4.87	1.46	5.50	1.65
	Average	4.46	1.78	5.95	1.78	6.76	2.03

Δ_s = additional deflection at column top due to shear deformation of beams and columns.

Many designers, particularly in the USA, model beam-column joints as rigid end zones in computer analysis. This is inappropriate and results in excessive stiffness [5] because of significant strain penetration of longitudinal reinforcement into the joint region. As a consequence, it is assumed herein that the yield curvature in the beam develops at the joint centroid, and reduces linearly to zero at the beam midspan, as shown in Fig. 3(c).

The yield drift θ_{by} due to beam flexure is thus

$$\theta_{by} = \frac{\phi_y\,(0.5\ell_b)}{3} = \phi_y \ell_b / 6 \qquad (8)$$

TABLE 2: EFFECTIVE STIFFNESS RATIOS

FOR DIFFERENT BEAM REINFORCEMENT DETAILS

REBAR	CASE	f_y =300 MPa		f_y =400 MPa	
		M_n (kNm)	I_e / I_g*	M_n (kNm)	I_e / I_g*
0.82% top & bottom, single layer	-ve	244	0.170	324	0.151
	+ve	256	0.190	340	0.173
	Average		0.180		0.162
1.54% top & bottom, single layer	-ve	447	0.291	591	0.299
	+ve	469	0.347	622	0.361
	Average		0.319		0.330
2.2% top & bottom, single layer	-ve	632	0.392	838	0.397
	+ve	661	0.492	877	0.493
	Average		0.442		0.445
2.2% top & bottom, two layers	-ve	590	0.342	795	0.350
	+ve	646	0.433	851	0.458
	Average		0.338		0.404
2.2% top (two layers) 1.1% bottom (one layer)	-ve	603	0.331	778	0.320
	+ve	354	0.279	465	0.276
	Average		0.305		0.298

NOTE: *Based on E = 30 GPa, $I_g = 0.01155 m^4$

Ignoring strain hardening and thus substituting from Eqn.(4a):

$$\theta_{by} = 0.283\, \varepsilon_y \left[\frac{\ell_b}{h_b}\right] \qquad (9)$$

Typical calculations based on a storey height/bay length ratio of 0.533 (storey height = 3.2 m, bay length = 6 m) and a maximum column curvature of $0.75\phi_y$ indicate column displacement Δ_c will add about 40% to the yield drift in Eqn. (7). It is further assumed, based on experience, that the joint deformation and member shear deformation add 25% and 10% respectively to the yield drift. As a consequence, the yield drift is predicted to be

$$\theta_y = (1+0.4+0.25+0.1)\times 0.283\, \varepsilon_y \left[\frac{\ell_b}{h_b}\right] = 0.5\, \varepsilon_y \left[\frac{\ell_b}{h_b}\right] \qquad (10)$$

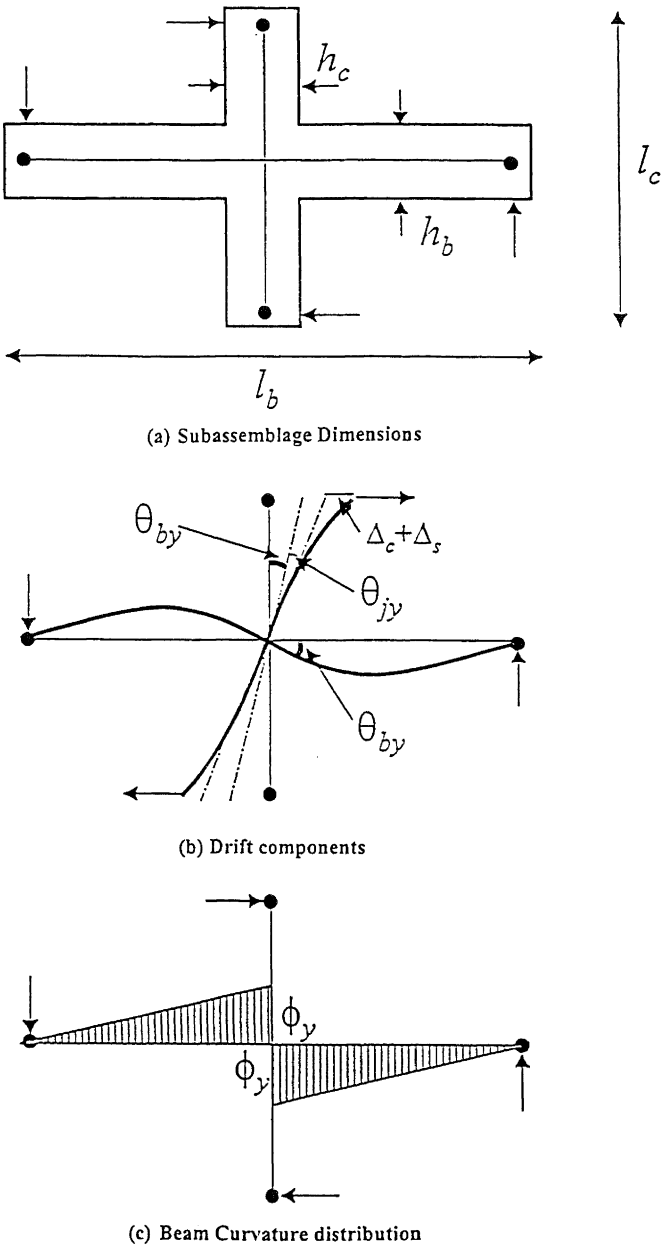

Figure 3: Approximate elastic drift calculations for beam/column joint subassemblages

In order to examine the applicability or otherwise of Eqn. (10), yield drifts it predicted were compared with measured yield drifts from 46 beam/column subassemblage experiments [6-23].

These experiments were mainly of interior beam/column joints, but also included a few exterior joints, since Eqn. (10) should also be applicable for exterior joints. The experiments included a wide range of possibly relevant parameters, including:

Column height / beam length aspect ratio (ℓ_c/ℓ_b) : 0.4- 0.86

Concrete compression strength (f'_c) : 22.5 - 88 MPa

Beam reinforcement yield strength (f_y) : 276 – 611 MPa

Maximum beam reinforcement ratio ($A_s' / b_w d$)

: 0.53% - 3.9%

Column axial load ratio ($N_u / f_c' A_g$) : 0 - 0.483

Beam aspect ratio (ℓ_b / h_b) : 5.4 - 12.6

Designs with equal, and with unequal top and bottom beam reinforcement where considered, as were designs with and without slabs and/or transverse beams. A few possible tests were excluded [24-26] because of lack of joint reinforcement and/or unacceptably small ratios of column depth h_c to beam bar diameter d_b, which resulted in excessive joint deformation or beam bar slip, respectively. These experiments resulted in yield deformation which would not be realistic for modern designs. A further possible test series [27] was discarded because of apparent displacement anomolies in the critical small-deformation range.

Relevant test details are listed in Table 3, together with the predicted yield drift θ_T based on Eqn. (9), and the experimentally observed yield drift θ_E . In all cases, yield strain was based on reported yield stress f_y and an assumed modulus of elasticity of E_s = 200 GPa. Where different bar sizes in a given section resulted in variation in f_y, an average value was used.

Table 3 also includes the ratio of θ_E / θ_T. An average value of θ_E/θ_T = 1.03, with a standard deviation of 0.16 was obtained. Considering the wide range of parameter considered, this comparitively narrow scatter is rather satisfactory. As may be seen from Fig.4, which plots θ_E against θ_T, the agreement is reasonable over the full range of yield drifts. It should be noted that the two largest experimental drifts, corresponding to Menheit and Jirsa's [17] tests II and VI are likely to include significant bar slip deformation as a consequence of the low h_c/d_b ratio, and comparitively high yield strength.

In order to examine sensibility to different potentially significant parameters, the experiment/prediction ratio θ_E/θ_T is plotted against reinforcement yield strength, concrete compression strength, maximum beam tension reinforcement ratio, beam aspect ratio (ℓ_b/h_b), test unit aspect ratio (ℓ_c/ℓ_b) and column axial load ratio, in Figs. 5-10. In no figure is a strong trend apparent, though there appears to be a trend for θ_E/θ_T to increase with test unit aspect ratio, and with beam reinforcement ratio, and to decrease with beam aspect ratio increase. These are expected, since increased relative column height will increase the contribution of column deformation to the yield drift, and the analyses reported in Tables 1 and 2 predict increased yield curvature for increased reinforcement ratios, and shear deformation will increase for low ℓ_b / h_b ratios.

SIGNIFICANCE OF RESULTS

The significance of the invariance of dimensionless yield curvature with strength has already been pointed out. In force-based designs the assumption of member stiffness as a constant fraction of gross stiffness, regardless of strength, can lead to significant errors in period and deformation calculations. Note that Fig.7 indicates that tension stiffening effects, which might be expected to reduce experimental drift ratios below predicted values for beam reinforcement ratios lower than ρ = 0.01, does not appear to be significant. In most cases, structural stiffness will be less than assumed. This will particularly be the case if rigid end zones are included in the analysis, and if joint deformation is ignored, which will almost always be the case. The consequence will be that structures may be designed for too high a base shear force, because of the low estimated period, but displacements will be underpredicted, leading to the possibility of excessive non-structural damage.

It is of interest to investigate the probable levels of yield drift to be expected in modern design. Examination of results in Table 3 indicates a range from 0.44% to 1.5%. However, many of the test units of Table 3 have proportions that would be considered unusual for current design. If we consider a minimum probable bay length of 6.0 m, and a typical beam depth of 600 mm, then Eqn. (9) will predict a yield drift of 0.75% and 1.00% for frames with beams reinforced with grade 300 and grade 400 reinforcement, respectively.

The New Zealand loadings code [28] permits a maximum interstorey drift of 2.0% for $h_n \leq$ 15m and 1.5% for $h_n >$ 30, where h_n is the total building height, with linear interpolation between, unless drift is checked with inelastic time-history analysis, in which case a predicted drift of 2.5% is permitted, regardless of height. It should be noted that 2.5% drift is larger than permitted by several overseas codes (e.g. 29) where limitations are imposed to reduce potential non-structural damage.

The consequence of these limits is that even for the comparatively squat example considered, the storey drift demand must be less than μ = 2.7 or 2.0 for f_y = 300 and 400 MPa, respectively, for designs based on elastic analyses procedures, and μ = 3.3 and 2.5 for f_y = 300 and 400 MPa, respectively, when the design is checked by inelastic time-history analyses. It should be noted that the structural displacement ductility will always be less than the ductility demand of the critical story, and hence design displacement ductility levels should be less than these values.

As a consequence, it will almost never be possible to make use of the full displacement ductility capacity of μ = 6 permitted by the concrete code [3] for fully ductile frames. Adopting a minimum bay length of 6 m, a beam depth of 1.3 m would be necessary to obtain a structure with sufficient elastic stiffness to achieve a displacement durability of μ = 6 before reaching the code drift limitations.

Consider the implications to current force-based design. Imagine a structure with an elastic period of (say) 1.2 seconds based on conventional stiffness estimates. Based on design to a displacement ductility of μ = 6, it is found that the maximum drift just reaches the code limit of 2.0%. Imagine further, that analysis based on the method developed in this paper indicates that the elastic structural stiffness is too high by a factor of 2. This would be a common result.

TABLE 3: COMPARISON OF MEASURED & PREDICTED YIELD DRIFTS OF BEAM/COLUMN SUBASSEMBLAGES

Refer -ence	Unit No.	ℓ_b (mm)	ℓ_c (mm)	$\frac{\ell_c}{\ell_b}$	h_b (mm)	$\frac{\ell_b}{h_b}$	f'_c (MPa)	f_y (MPa)	(max) θ_t	$\frac{N_u}{f'_c A_g}$	θ_T	θ_E	$\frac{\theta_E}{\theta_T}$
6	B11	4420	2744	0.621	610	7.25	35.9	298	0.0084	0.043	0.0054	0.0063	1.17
	B12	4420	2744	0.621	610	7.25	34.6	298	0.0063	0.045	0.0054	0.0063	1.17
	B13a	4420	2744	0.621	610	7.25	31.4	298	0.0063	0.442	0.0054	0.0044	0.81
	B21	4420	2744	0.621	610	7.25	35.0	298	0.0069	0.442	0.0054	0.0047	0.91
7	B1	4880	3430	0.703	610	8.0	27.9	288	0.0128	0.053	0.0058	0.0085	1.47
	B2	4880	3430	0.703	610	8.0	31.5	288	0.0128	0.439	0.0058	0.0060	1.03
8	1D-I	4055	3500	0.863	550	7.37	38	292	0.0153	0.01	0.00538	0.00519	0.96
	2D-I	4055	3500	0.863	550	7.37	37	292	0.0153	0.01	0.00538	0.00541	1.01
	2D-E	4055	3500	0.863	550	7.37	38	292	0.0153	0.01	0.00538	0.00483	0.90
9	#3	4880	3354	.687	457	10.7	37.2	298	0.0188	0.216	0.00763	0.00768	1.01
10	U-1EXT	(2210)	3430	.776	610	7.25	22.6	298	0.0096	0.01	0.0054	0.00489	0.91
	U-2EXT	(2210)	3430	.776	610	7.25	22.5	298	0.0185	0.01	0.0054	0.0057	1.06
	U-3EXT	(2210)	3430	.776	610	7.25	26.9	298	0.0096	0.01	0.0054	0.00489	0.91
11	1	2667	2240	0.840	700	3.81	29	313	0.0079	0.01	0.0030	0.0043	1.43
	2	2667	2240	0.840	700	3.81	33	313	0.0079	0.01	0.0030	0.0036	1.20
	3	2667	2240	0.840	700	3.81	38	307	0.0082	0.01	0.0029	0.0034	1.17
	4	2667	2240	0.840	700	3.81	35	313	0.0220	0.01	0.0030	0.0039	1.30
	5	3810	2800	.735	700	5.44		320	0.0158	0.01	0.00435	0.0059	1.35
	6	3810	2800	.735	700	5.44		285	0.0105	0.01	0.00415	0.0049	1.19
12	U1	4418	2470	.559	457	9.7	45.6	294	0.0105	0.01	0.0071	0.0061	0.86
	U2	4418	2470	.559	457	9.7	36.0	306	0.0128	0.01	0.0074	0.0080	1.08
	U3	4418	2470	.559	457	9.7	36.2	294	0.0105	0.01	0.0071	0.0058	0.82
	U4	4418	2470	.559	457	9.7	36.2	306	0.0128	0.01	0.0074	0.0073	0.99
13	-	1950	1500	.769	250	7.8	43.5	369	0.0116	0.047	0.00722	0.0089	1.23
14	HN01	2800	1800	.643	400	7.0	88	610.5	0.0165	0.167	0.0107	0.0085	0.79
	HN03	2800	1800	.643	400	7.0	88	441	0.0390	0.167	0.0077	0.0090	1.17
	NO43	2800	1800	.643	400	7.0	54	382	0.0110	0.200	0.00665	0.0060	0.90
	NO47	2800	1800	.643	400	7.0	54	382	0.0110	0.200	0.00665	0.0060	0.90
15	-	2650	1625	.613	400	6.63	44.9	340	0.0275	0.210	0.00563	0.0056	1.00
16	-	4258	3658	.859	460	9.3	83.2	470	0.0127	0.01	0.0109	0.0119	1.09
17	II	4877	3658	.750	457	10.7	41.8	448	0.0211	0.254	0.012	0.0153	1.28
	VI	4877	3658	.750	457	10.7	36.8	448	0.0211	0.483	0.012	0.0146	1.22
	XII	4877	3658	.750	457	10.7	35.7	448	0.0211	0.300	0.012	0.0122	1.02
18	-	5740	3350	.584	457	12.6	41.3	315	0.0175	0.100	0.0104	0.00989	1.05
19	C1	2700	1470	.544	300	9.0	25.6	320	0.0159	0.077	0.00784	0.00734	0.94
	C2	2700	1470	.544	300	9.0	25.6	320	0.0159	0.077	0.00784	0.00816	1.04
	C3	2700	1470	.544	300	9.0	25.6	320	0.0159	0077	0.00784	0.00734	0.94
20	-	8600	3435	.399	889	9.7	48.5	276	0.0137	0.03	0.00668	0.00646	0.97
21	-	5740	3350	.584	457	12.6	34	338	0.0173	0.237	0.0106	0.0104	0.98
22	-	3658	1828	.50	457	8.0	31.1	491	0.0131	0.361	0.00983	0.00940	0.96
23	1	3500	2470	.706	500	7.0	30.9	453	0.0069	0.01	0.00793	0.00850	1.07
	2	3500	2470	.706	500	7.0	40.8	445	0.0070	0.01	0.00779	0.00670	0.86
	3	3500	2470	.706	500	7.0	42.5	445	0.0070	0.01	0.00779	0.00690	0.89
	4	3500	2470	.706	500	7.0	47.2	445	0.0053	0.01	0.00779	0.00580	0.75
	5	3500	2470	.706	500	7.0	60.7	492	0.0082	0.01	0.00861	0.0078	0.90
	6	3500	2470	.706	500	7.0	59.3	463	0.0107	0.01	0.00810	0.0070	0.86

As a consequence, the actual elastic period would be $\sqrt{2}$ times the predicted value, and equal to 1.7 seconds. In the medium period range, the design spectra of NZS4203 [28] are based on the assumption of constant spectral velocity. As a consequence, the displacement will be $\sqrt{2}$ times the code limit, or 2.83%, and the ductility demand will be $\mu = \Delta_u/\Delta_y = \sqrt{2} \times 6/2 = 4.24$.

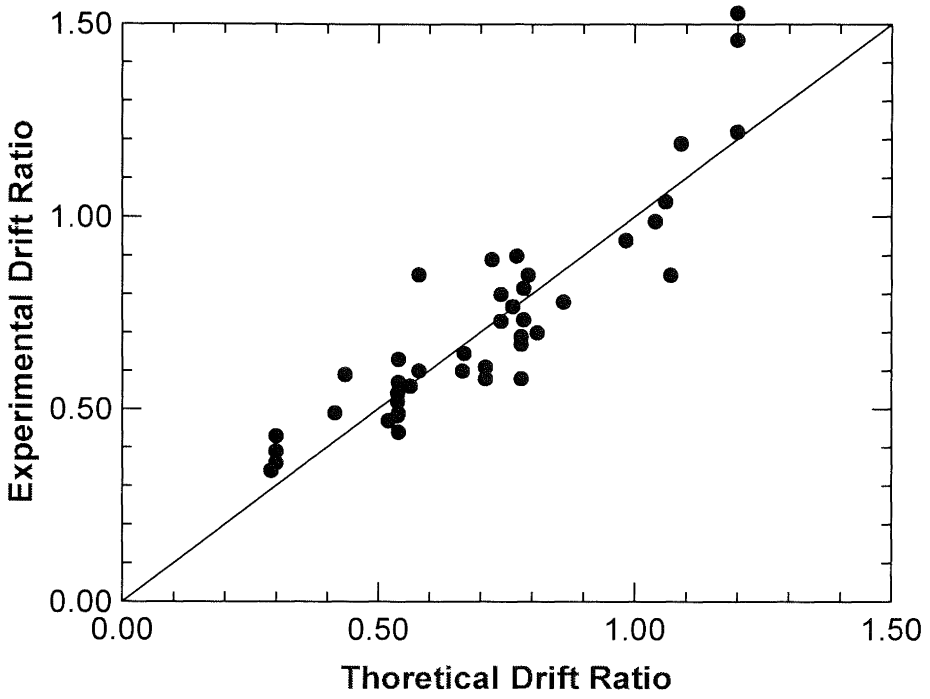

Figure 4: Experimental drift versus theoretical drift

Thus current frame designs are likely to have lower ductility demands than expected, but higher drifts. The consequence of this should be reduced structural damage, but increased non-structural damage.

Code provisions for maximum drift resulting from elastic analysis computations can be used to develop an approximate expression for the design displacement ductility factor that should be adopted. Thus, if θ_c is the code drift limit, then

$$\mu_D = \frac{\theta_c}{0.5\,\varepsilon_y}\left[\frac{h_b}{\ell_b}\right] \qquad (11)$$

where $\theta_c = 0.02$ for $h_n < 15$ m, 0.015 for $h_n > 30$ m,

and $\theta_c = 0.02 - 0.005\,(h_n - 15)\,/\,30$ for $15 \le h_n \le 30$ m

Although this will indicate an appropriate design ductility level for force-based design, it does not help with determining initial stiffness for initial period calculations, and it would appear that an iterative solution would be necessary based on an initial stiffness assumption. The alternative is to use displacement-based design principles rather than a force-based approach [4].

CONCLUSIONS

Analyses of typical beam designs for seismic resistant frames indicate that a dimensionless yield curvature could be determined that was insensitive to longitudinal reinforcement ratio or direction of loading. The consequence is that the beam stiffness is proportional to strength, and that the common assumption of a beam stiffness equal to a constant fraction of the gross stiffness is inappropriate for design. This has severe implications for force-based design.

Based on these analyses, a simple equation predicting the yield drift ratio of frames, depending only on the beam aspect ratio and reinforcement yield strain was proposed. When calibrated against a wide range of beam/column joint test data, good average agreement was obtained with a low coefficient of variation.

Results of the analysis indicated that the structural stiffness of frames is likely to be much lower than typically assumed by designers. A consequence is that most frame structures will exceed code drift limitations before achieving displacement ductility of $\mu = 4$. Only in the case of very deep-membered peripheral frames will the full permitted design ductility factor of $\mu = 6$ be achievable without violating code drift limits.

This result points to the irrationality of force-based design, since displacement criteria will almost always govern. An approximate value for the appropriate ductility factor for force-based design was developed.

On the other hand, the possibility of developing a dimensionless yield drift generally facilitates displacement-based design since the known ductility factor corresponding to the ultimate drift limitation implies that the appropriate level of damping can be determined with confidence before design details are obtained. This aspect is developed further elsewhere [4].

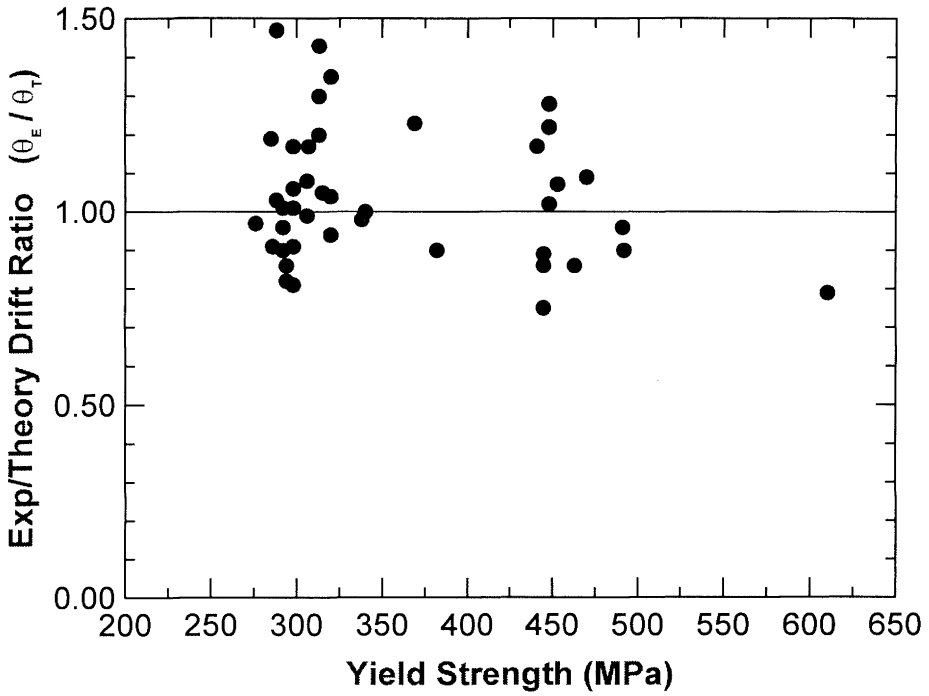

Figure 5: Influence of beam reinforcement yield strength on (θ_E/θ_T) ratio

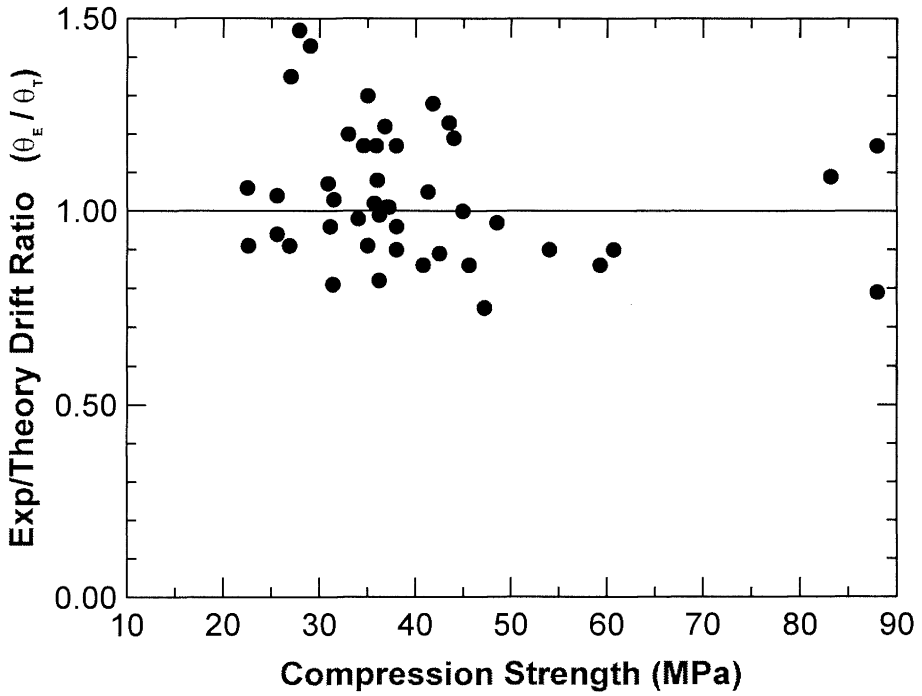

Figure 6: Influence of concrete compression strength (f_c') on (θ_E/θ_T) ratio

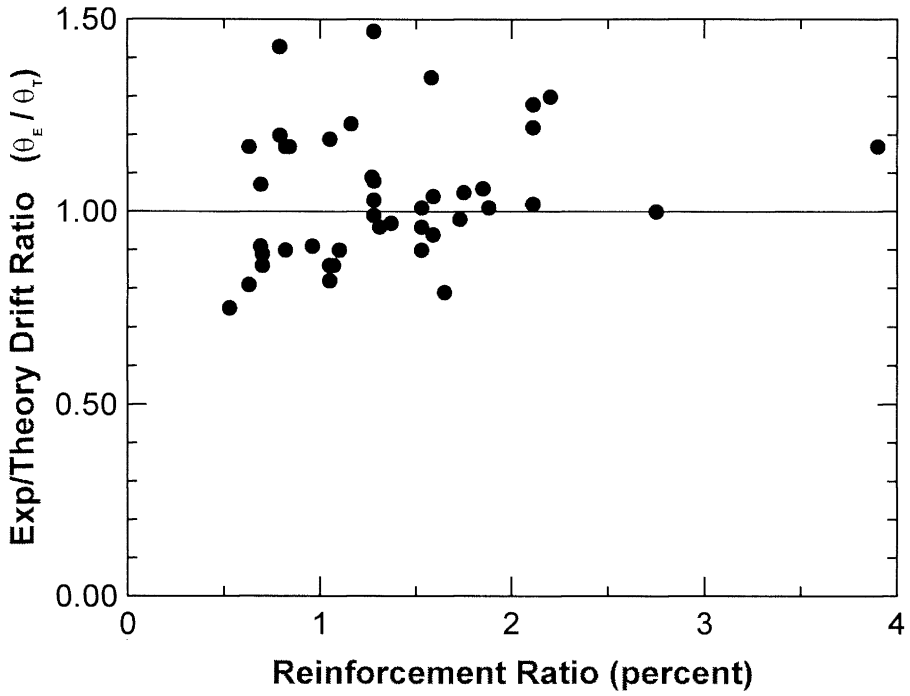

Figure 7: Influence of beam top reinforcement ratio (ρ_t) on (θ_E/θ_T) ratio

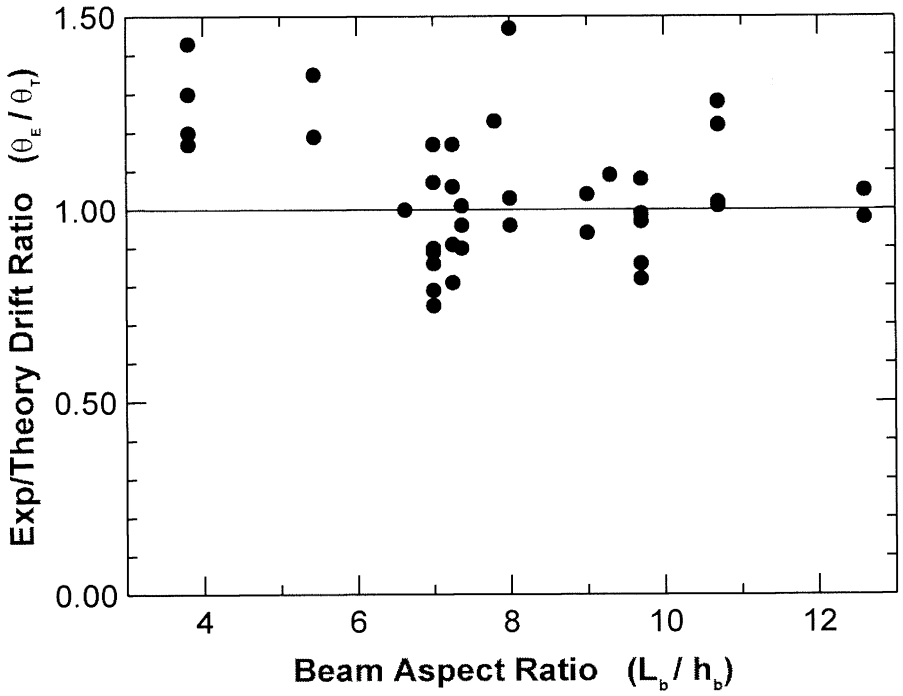

Figure 8: Influence of beam aspect ratio (Length/Depth) on (θ_E/θ_T) ratio

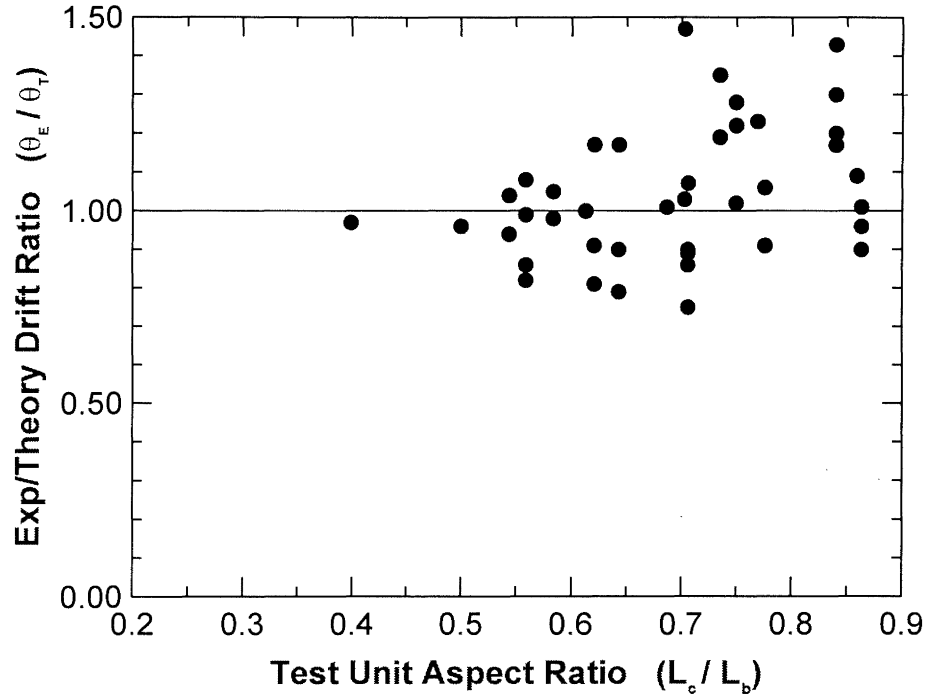

Figure 9: Influence of test unit aspect ratio on (θ_E/θ_T) ratio

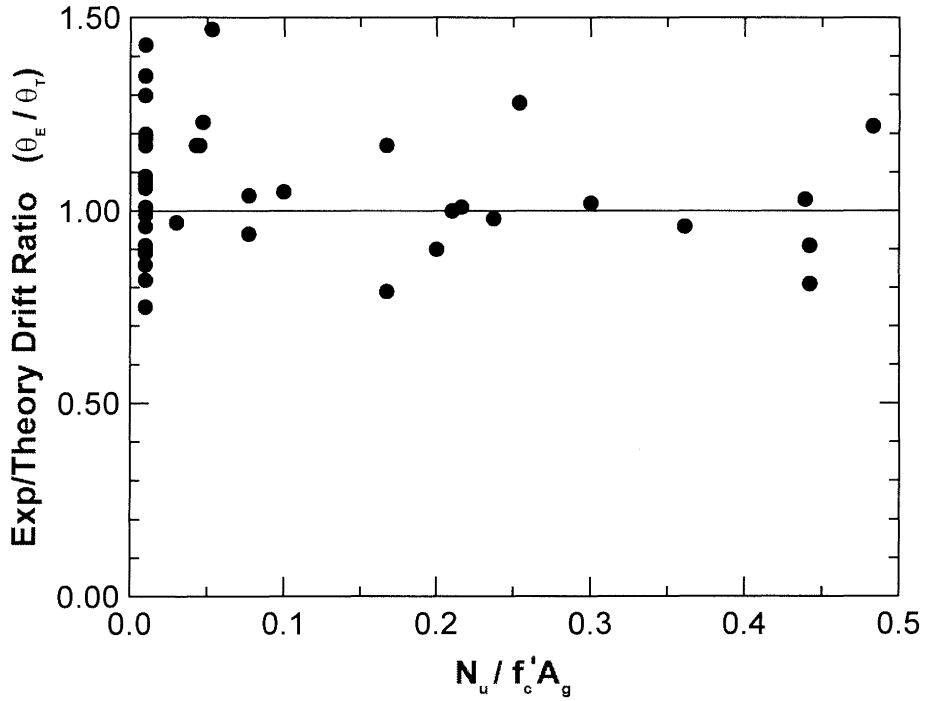

Figure 10: Influence of column axial load ratio on (θ_E/θ_T) ratio

The results presented in this paper apply to modern designs with adequate joint reinforcement and suitable column depth / bar diameter ratios. They should not be applied to assessment of pre 1970's buildings, which are likely to be significantly more flexible than predicted by the equation as developed herein.

ACKNOWLEDGEMENTS

Much of the data of Table 3 used to calibrate the yield drift model came from a data base collected by C.M. Lin & Dr. José Restrepo of the University of Canterbury. Their generous gift of access to this information is greatly appreciated. Financial assistance of the EQC through its distinguished Earthquake Research Fellowship is gratefully acknowledged.

REFERENCES

1. Priestley, M.J.N., Seible, F., and Calvi, G.M. (1996), Seismic Design and Retrofit of Bridges, *John Wiley & Sons, NY*, 686pp.

2. Priestley, M.J.N., and Kowalsky, M.J. (1998), Aspects of Drift and Ductility Capacity of Rectangular Cantilever Structural Walls, *Bulletin, NZNSEE*, June ,pp 73-85.

3. SANZ (1995) NZS3101: 1995 – Concrete Structures Standard, *Standards New Zealand, Wellington* [2 Vols: Code & commentary].

4. Priestley, M.J.N. and Calvi, G.M. (1997), Concepts and Procedures for Direct Displacement Based Design and Assessment *Proc. International Conference on Seismic Design Methodologies for the next generation of Codes.* Pub. A.A. Balkema, Rotterdam, pp 171-182.

5. Paulay, T. and Priestley, M.J.N. (1992), Seismic Design of Reinforced Concrete and Masonry Structures, *John Wiley & Sons, NY,* 744 pp.

6. Beckingsale, C.W. (1980), Post-elastic Behavior of Reinforced Concrete Beam – Column Joints, Research Report 80-20, *Dept. of Civil Engineering, University of Canterbury,* 398 pp.

7. Birss, G.R., Paulay, T. and Park, R. (1978), The Elastic Behavior of Earthquake Resistant Reinforced Concrete Interior Beam Column Joints, Research Report 78-13, *Dept. of Civil Engineering, University of Canterbury,* Christchurch, 96pp.

8. Cheung, P.C., Paulay, T., and Park, R. (1991), N.Z. Tests on Full-scale Reinforced Concrete Beam-Column-Slab Subassemblages Designed for Earthquake Resistance, In "Design of Beam-Column Joints for seismic Resistance", James O. Jirsa, Ed. Special publication SP123, *American Concrete Institute, Detroit,* pp. 1-38.

9. Thompson, K.J. and Park, R. (1974), Behaviour of Prestressed, Partially Prestressed and Reinforced Concrete Interior Beam-Column Assemblies under Cyclic Loading: Test Results of Units 1-7, Research Report 74-9, *Dept. of Civil Engineering, University of Canterbury,* Christchurch, 42pp.

10. Paulay, T. and Scarpas, A. (1981), The Behaviour of Exterior Beam-Column Joints, *Bulletin, NZNSEE*, Vol. 16, No.1, March, pp. 131-144.

11. Restrepo-Posada, J.I., Park, R., and Buchanan, A.H. (1993), Seismic Behaviour of Connections Between Precast Concrete Elements, Research Report 93-3, *Department of Civil Engineering, University of Canterbury,* Christchurch, NZ, 385 pp.

12. Dai, R. and Park, R. (1987), A Comparison of the Behavior of Reinforced Concrete Beam-Column Joints Designed for Ductility and Limited Ductilty, Research Report 87-4, *Dept. of Civil Engineering University of Canterbury,* 65pp.

13. Fujui, S. and Morita, S. (1989), Behavior of Exterior R.C. Beam-Column –Slab Subassemblages under Bi-directional Loadings, *Proc. 3rd US-NZ-Japan-China Seminar on Design of R.C. Beam Column Joints for Earthquake Resistance*, Christchurch, 12 pp.

14. Teraoka, M., Kanoh, Y., Taraka, K., and Hayoshi, K. (1994), Shear Strength and Deformation Behavior of R.C. Interior Beam-Column Joint Using High Strength Concrete, *Proc. 2nd US-NZ-Japan-China Multilateral Meeting on structural Performance of High Strength Concrete in Seismic Regions.* Honolulu.

15. Bessho, S., Fukushima, M., and Hatamoto, H. (1995), Behavior of Reinforced Concrete Beam-Column Joints, Research Report, *Kajima Institute of Construction Technology,* May.

16. Lawrence, G.M. and Beattie, G. (1993), The cyclic Load Performance of a High Strength Concrete Beam-Column Joint, *Central Laboratories Report 93-25130,* Lower Hutt, New Zealand, 50 pp.

17. Meinheit, D.F. and Jirsa, J.O. (1997), The Shear Strength of R.C. Beam Column Joints, CESRL Report 77-1, *Dept. of Civil Engineering, University of Texas at Austin.*

18. Milburn, J.R. and Park, R. (1982), Behaviour of R.C. Beam-Column Joints Designed to NZS3101, Research Report 82-7, *Dept. of Civil Engineering, University of Canterbury,* Christchurch, 107 pp.

19. Otani, S., Kitayama, K., and Aoyama, H. (1985), Beam Bar Bond Stress and Behavior of Reinforced Concrete Interior Beam-Column Connections, *Proc. 2nd US-NZ-Japan Seminar on Design of R.C. Beam-Column Joints, Tokyo,* 40 pp.

20. Priestley, M.J.N. (1975), Testing of Two R.C. Beam-Column Assemblies Under Simulated Seismic Loading. Report 5-75/1, *Central Laboratories,* Lower Hutt, NZ, 114 pp.

21. Stevenson, E.C. (1980), Fibre Reinforced Concrete in Seismic Regions, M. Eng. Thesis, *Dept. of Civil Engineering, University of Canterbury*, Christchurch.

22. Viwathanatepa, S., Popov, E.P. and Bertero, V.V. (1979), Seismic Behavior of R.C. Interior Beam-Column Subassemblages, Report UCB/EERC-79/14, *Earthquake Engineering Center, University of California, Berkeley,* 184 pp.

23. Xian Zuo, X., Park, R., and Tanaka, H. (1992), Behaviour of R.C. Interior Beam-Column Joints Designed Using High Strength Concrete and Steel, Research Report 92-3, *Dept. of Civil Engineering, University of Canterbury,* Christchurch, 121 pp.

24. Durani, A.J. and Wight, J.K. (1982), Experimental and Analytical Study of Internal Beam to Column Connections Subjected to Reversed Cyclic Loading, Report UmEE82R3, *Dept. of Civil Engineering, University of Michigan,* Ann Arbor, 275 pp.

25. Hakuto, S., Park, R., and Tanaka, H. (1994), Behaviour of As-Built and Retrofitted Beam-Column Joints of a 1950's Designed R.C. Building Frame, *Proc. Technical Conference of NZNSEE,* Wairakei, pp. 16-27.

26. Otani, S., Kobayashi, Y., and Aoyama, H. (1984), Reinforced Concrete Interior Beam-Column Joints Under Simulated Earthquake Loading, *Proc. 1st US-NZ-Japan Seminar on Beam-Column Joints,* Monterey, July.

27. Joh, O., Goho, Y., and Shibata, T. (1981), Influence of Transverse Joint and Beam Reinforcement and Relocation of Plastic Hinge Region on Beam-Column Joint Stiffness Determination, in "Design of Beam-Column Joints for Seismic Resistance." James O. Jirsa, Ed. *ACI SP-123 American Concrete Institute,* Detroit, pp. 187-223.

28. NZS 4203:1992, Code of Practice for General Structural Design and Design Loadings for Buildings, *Standards New Zealand,* 134 pp.

29. UBC 1997, Uniform Building Code, *International Conference of Building Officials,* Whittier, California.